

Measurement of hardness, surface potential, and charge distribution with dynamic contact mode electrostatic force microscope

J. W. Hong, Sang-il Park,^{a)} and Z. G. Khim^{b)}

Department of Physics and Condensed Matter Research Institute, Seoul National University, Seoul 151-742, Korea

(Received 21 August 1998; accepted for publication 30 November 1998)

Dynamic contact mode electrostatic force microscopy (DC-EFM) was developed as a new operation mode of scanning probe microscope (SPM). By operating EFM in a contact mode with an ac modulation bias, we have improved the spatial resolution and also achieved a complete separation of the topographic effect from other electrostatic force effect overcoming the mixing problem of a topographic effect with other electrostatic effects frequently encountered in the conventional noncontact EFM measurement. DC-EFM can be utilized either as a force microscopy for the surface hardness, or as a potentiometry for the surface potential distribution, or as a charge densitometry for the surface charge density study. This is also applicable to the measurement and control of the domain structure in ferroelectric materials that have a bound surface charge. © 1999 American Institute of Physics. [S0034-6748(99)01703-7]

I. INTRODUCTION

Scanning probe microscope (SPM) has matured and developed into a routine instrument for the investigation of the surface topography of insulating as well as conducting samples with an atomic resolution. Recent efforts have revealed a much broader potential for the measurement of local mechanical properties¹ and electrical properties such as surface potential,²⁻⁴ surface charge,^{5,6} and ferroelectric domain⁷⁻⁹ by electrostatic force microscope (EFM).

Earlier force modulation microscopy (FMM) was achieved by applying a small mechanical sinusoidal force on the surface when the tip was close to the sample.¹ Unfortunately, in the earlier FMM technique, either sample or probe cantilever is vibrated with a mechanical transducer. In either case, the mechanical transducer has a rather poor amplitude versus frequency response of the probe usually exciting several unwanted modes of vibration and noise. To avoid this problem, we have successfully employed tapping mode using an electrostatic force modulation technique¹⁰ for the study of the surface morphology by applying an ac modulation signal to the tip instead of the mechanical modulation force using a bimorph.

Conventional EFM is usually operated in a dynamic noncontact mode,¹¹ where the change of the vibration amplitude due to a force gradient is used to detect the variation of the force gradient due to either topography or other interactions. Therefore, in the dynamic noncontact EFM, it is difficult to separate the effect of topography from that of the other origin. For example, abrupt changes in the surface potential and surface charge on the sample surface produce a large electrostatic force gradient. In such cases, the probe tip cannot follow a true topography but a force gradient contour

including the electrostatic force gradient as well as van der Waals force gradient. Such a mixing of force gradients causes successive errors in measuring the electrical properties of the sample. In addition, the noncontact mode operation is rather complicated and its spatial resolution is significantly reduced compared to that of the contact mode operation, since the tip is far away, approximately 10 nm, from the surface.

We have overcome the problems of the conventional operation mode of EFM, and have successfully obtained images of surface topography, surface potential, and surface charge distribution by operating EFM in a contact mode with an ac electrostatic modulation, which we termed as dynamic noncontact mode EFM (DC-EFM)¹² to distinguish it from the conventional noncontact mode EFM.

In this report, we will explain the detection principle of DC-EFM for the measurement of the surface hardness, surface potential distribution, and surface charge density. Ferroelectric domain image obtained by DC-EFM is compared with that obtained by the conventional noncontact operation of EFM.

II. DETECTION METHOD

In DC-EFM, a contact mode atomic force microscope (AFM) is employed to maintain the tip-sample distance constant. A dc and ac bias voltage is applied between the conductive probe tip and sample in the contact mode. The probe tip used in this work is a heavily doped Si (doping level is 10^{19} – $10^{20}/\text{cm}^3$) with a spring constant $k=1.9\text{ N/m}$ and a typical tip radius $R=20\text{ nm}$. An insulating layer on the probe tip such as native oxide layer prevents electrical current flowing between the tip and sample.

The idea behind DC-EFM operation is, first, to utilize the *sustained vibration* of the cantilever even in the contact state, when an ac electrostatic modulation signal is applied to the tip. That is, even when the tip is in contact with the

^{a)}Present address: PSIA Corp., Daelim Bldg., Seocho-dong 1600-3, Seoul 137-070, Korea.

^{b)}Electronic mail: jnine@plaza.snu.ac.kr

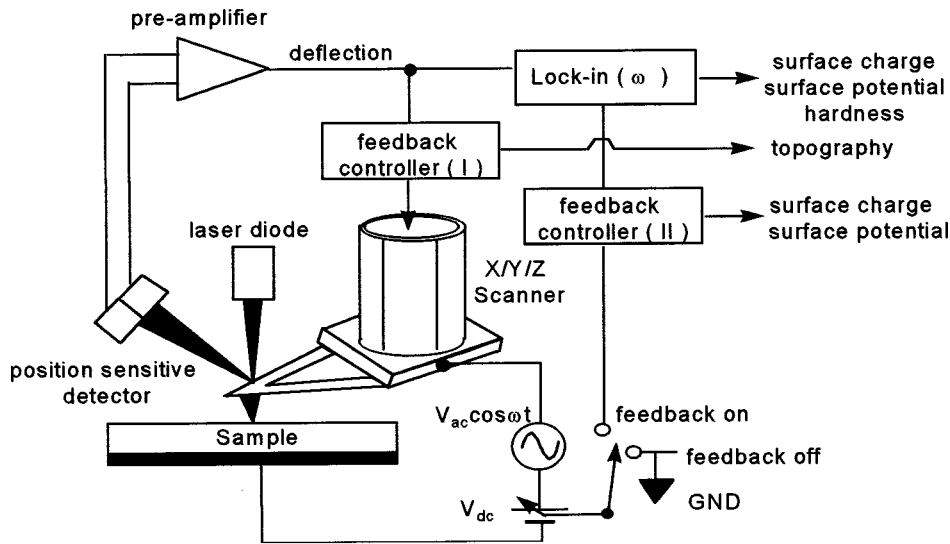


FIG. 1. Schematic diagram of DC-EFM. With the lock-in amplifier feedback off, output of lock-in amplifier can be used for the detection of surface potential or surface charge density. For the estimate of the absolute value of surface potential or the surface charge density, one can measure the lock-in feedback signal that controls V_{dc} such that the amplitude of ω component (lock-in amplifier output) vanishes.

sample surface, there still remains a finite vibration amplitude of the probe tip. The sustained vibration of the tip in a contact state was already confirmed in the force microscope.¹ Then even in the presence of a strong atomic force in the contact mode, a weak electrostatic interaction between tip and sample surface can be detected by a lock-in technique. Second, by applying a bias to the tip one can for example control the induced charge on the tip, which in turn generates an additional controllable force between the tip and charged surface. Therefore we can simultaneously measure the topography and other electrostatic interaction effect such as surface potential or surface charge density with DC-EFM.

The general equation describing the force between the tip and sample at a surface position \mathbf{r} in the presence of surface potential or surface charge density includes atomic force, capacitive force, and Coulombic force between the charge induced on the tip and sample surface charge:

$$F(\mathbf{r}) = F_a(\mathbf{r}) + 1/2 \partial C(\mathbf{r}) / \partial z V^2 + E_s(\mathbf{r}) q_{\text{tip}}. \quad (1)$$

Here, F_a represents the repulsive atomic force on the tip. In the capacitive force term, $\partial C / \partial z$ is the gradient of capacitance between tip and sample, which depends on the tip-sample geometry. The potential V between the tip and sample surface may contain external dc bias V_{dc} and ac bias $V_{ac} \cos \omega t$ as well as the sample surface potential V_s . $E_s(\mathbf{r})$ and $q_{\text{tip}} = C(V_{dc} + V_{ac} \cos \omega t)$ represent the electric field generated by the surface charge density of the sample and the charge induced on the tip, respectively.

With $V = (V_{dc} - V_s + V_{ac} \cos \omega t)$ and $q_{\text{tip}} = C(V_{dc} + V_{ac} \cos \omega t)$, the force on the tip reduces to

$$\begin{aligned} F(r) &= F_a(r) + 1/2 \partial C(r) / \partial z (V_{dc} - V_s + V_{ac} \cos \omega t)^2 \\ &\quad + E_s(r) C(r) (V_{dc} - V_s + V_{ac} \cos \omega t) \\ &= [F_a(r) + 1/2 \partial C(r) / \partial z (V_{dc} - V_s)^2 \\ &\quad + 1/4 \partial C(r) / \partial z V_{ac}^2 + E_s(r) C(r) (V_{dc} - V_s)] \\ &\quad + [\partial C(r) / \partial z (V_{dc} - V_s) + E_s(r) C(r)] V_{ac} \cos \omega t \\ &\quad + 1/4 \partial C / \partial z V_{ac}^2 \cos 2 \omega t. \end{aligned} \quad (2)$$

Since DC-EFM is operated in the contact mode, the dc component of the force (static deflection of the cantilever) is adjusted by the z servoloop such that the strong repulsive atomic force between tip and surface is maintained constant. Thus, the dc component provides the topographic image as in the conventional contact mode operation of AFM. On the other hand, the detection of the ω component, $[\partial C / \partial z (V_{dc} - V_s) + E_s C]$, can provide information about V_s or E_s depending on the experimental situation.

Now if the sample surface is not sufficiently hard and has variations in its hardness, then the surface may have certain compliance due to electrostatic force modulation. Therefore a strong electrostatic force can drive the probe tip to vibrate by indenting the sample surface. The vibration amplitude will depend on the surface hardness and the strength of the electrostatic force. In this case, the capacitance (or the gradient of the capacitance) between the tip and sample will show a dependence on the surface hardness. We can write the relationship between the hardness and relative amplitude of the tip vibration as follows:

$$F(\mathbf{r}, \omega) = k_{\text{eff}}(\mathbf{r}, \omega) z(\mathbf{r}, \omega), \quad (3)$$

where $z(\mathbf{r}, \omega)$ represents the amplitude of the tip vibration at a position \mathbf{r} caused by the electrostatic force $F(\mathbf{r}, \omega)$. Thus in the absence of surface charge or potential distribution on the sample, we can approximate the electrostatic force to be constant over \mathbf{r} . Furthermore, by keeping the ac and dc bias at a constant value, we can determine the variation of the effective mechanical hardness k_{eff} by measuring the ω component of the electrostatic vibration,

$$k_{\text{eff}}(\mathbf{r}, \omega) = F(\mathbf{r}, \omega) / z(\mathbf{r}, \omega). \quad (4)$$

The lock-in amplifier was used to measure the vibration amplitude and phase of the probe at frequency ω . During this measurement, the dc part of the force is taken as the feedback signal to maintain a constant height in the contact mode operation thus avoiding any mixing of the topographic effect with the surface hardness effect.

Figure 1 shows a schematic diagram of the DC-EFM. The signal from the topographic feedback controller (z ser-

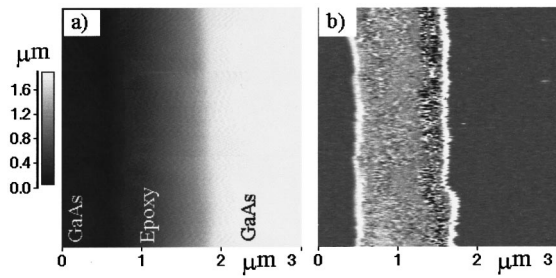


FIG. 2. Topography (a) and force modulation (b) image of a sample surface. Two hard GaAs regions are separated by a soft epoxy. The vibration amplitude at frequency ω force is much higher in soft epoxy than one in hard GaAs region.

vocontroller) that is to maintain the tip-sample height constant can be employed to image the surface morphology. With the feedback controller II off, the output of lock-in amplifier can be used for the detection of surface potential or surface charge density. For the estimate of the absolute value of surface potential or the surface charge density, one can measure the feedback controller II signal that controls V_{dc} such that the amplitude of ω component (lock-in amplifier output) vanishes.

III. EXPERIMENTAL RESULTS

As an example of DC-EFM, operation for the mechanical hardness measurement, images of the GaAs/epoxy/GaAs multilayer were taken by DC-EFM. Two GaAs wafers are glued together by a soft epoxy layer at the center. Figure 2 shows topography [Fig. 2(a)] and hardness [Fig. 2(b)] images obtained simultaneously for a polished surface which has regions of different mechanical hardness. In this measurement, applied dc bias, amplitude of ac bias, and frequency were 1 V, 5 V, and 40 kHz, respectively. Topography image barely reveals three separated regions of GaAs-epoxy-GaAs layers. However, the image obtained by the ω component clearly shows three distinctively separated layers. Because the central epoxy region is softer than both sides of the GaAs region, the amplitude of probe vibration at frequency ω in epoxy region is larger than the one in GaAs region. Thus the ω component of the tip vibration due to an electrostatic force in DC-EFM reflects the local mechanical hardness of a sample surface.

There are advantages of using DC-EFM for the mechanical hardness measurement compared to the earlier FMM technique using a bimorph driven mechanical modulation. In the FMM mode, the mechanical modulation usually generates several vibration modes of the microscope system, which can cause some ambiguity in the measurement. However the electrostatic modulation vibrates only the cantilever without shaking the entire part of the scanning or supporting cantilever system. Thus, we can get a clean vibration spectra. As a result, DC-EFM can prevent mixing or coupling of a main signal with unwanted noise sources.

Now if there is a surface potential distribution V_s on the sample surface but in the absence of surface charge density, the ω component in Eq. (2) reduces simply to $\partial C/\partial z(V_{dc} - V_s)$. Therefore DC-EFM can be operated as a potentiom-

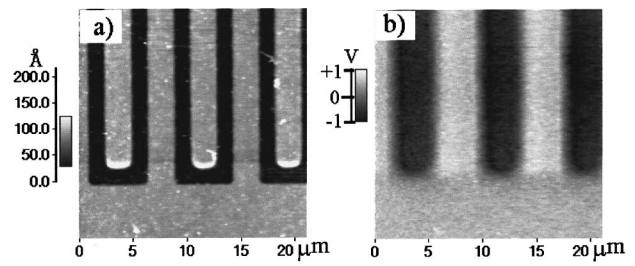


FIG. 3. Topography (a) and surface potential (b) image of an integrated test chip where one set of the trace is biased at +1 V and the other set of the trace is biased at -1 V.

etry by detecting the ω component in the presence of a surface potential $V_s(\mathbf{r})$ such as a pn junction or signal line in the integrated circuit. In order to measure the absolute value of the surface potential, a feedback loop is used to adjust the dc bias of the probe ($V_{dc,p}$) such that the vibration amplitude of the ω component vanishes.^{3,4} In this situation, the applied dc bias voltage to the probe is equal to the surface potential. An example is shown in Fig. 3, the topographic [Fig. 3(a)] and surface potential [Fig. 3(b)] image of a test pattern, where one set of the trace is biased at +1 V and the other set of the trace is biased at -1 V. A thin SOG layer was covered on the top of the sample surface. Thus we can assume that the surface hardness is uniform through the entire surface. In the topographic image, two metal lines (bright region) are separated by the etched insulating region. From the surface potential image, we can find that the line profile of the potential is changing linearly across the etched region as expected. The resolution of this potentiometry is about ~ 20 mV.

In another case, if the sample surface has a bound surface charge density σ_b , the electrostatic force is given as a sum of a capacitive force and Coulomb force between tip and sample. Since the probe tip-sample distance is very short in contact mode operation, one can approximate the effect of the bound surface charge density by a uniform surface electric field E_s . If the area of the bound charge is smaller than the effective area of the tip end, this approximation is no more valid. Thus the lateral resolution will be limited by the size of the tip radius. However, with 20 nm in tip radius, this approximation will be valid for the investigation of the ferroelectric domain structure because the domain size is usually much larger than the tip radius. In this approximation, Coulomb force can be expressed simply as $E_s q_t$, where $E_s = \sigma_b/2\epsilon_0$ is the electric field due to the constant surface charge density σ_b , and q_{tip} is the charge, $q_t = CV$, induced at the tip by the applied voltage $V = V_{dc} + V_{ac} \cos \omega t$.

Figure 4 shows the calculated electric field for ferroelectric strip domains with an alternating surface charge density $\pm \sigma_b$ and width $w = 2 \mu\text{m}$ which is a typical value for a triglycine sulfate (TGS) single crystal as a function of the position x and height z from the surface. For a tip height less than 10 nm, one can represent the effect of the surface charge density by a uniform surface electric field $E_s = \sigma_b/2\epsilon_0$ as we assumed above. A large electric field gradient appears near the domain boundary where two opposite charge densities collide. For a tip height greater than 10 nm, for example, a significant force gradient appears as shown in Fig. 4. Thus

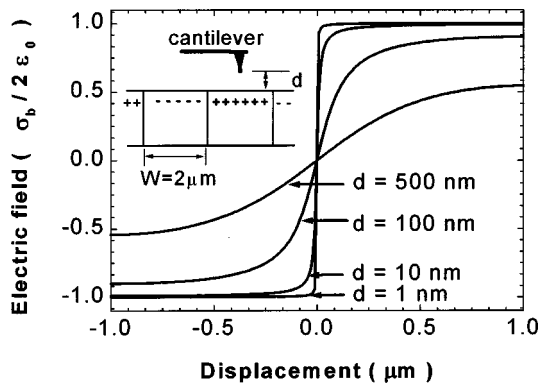


FIG. 4. Plot of electric field as function of lateral position on the alternating charge strip of width $2 \mu\text{m}$ at four different heights from surface.

the ω component of the electrostatic force in DC-EFM in the presence of a bound surface charge density becomes $(\partial C/\partial z V_{\text{dc}} + \sigma_b C/2\epsilon_0)$ which depends both on V_{dc} and the surface charge density σ_b . Therefore, measurements on the amplitude of the ω component of the cantilever vibration lead to the detection of the surface charge density or the domain image, in the case of a ferroelectric surface. The topographic image can be obtained from the feedback signal due to the repulsive atomic force (dc component) that maintains a constant tip height (or a constant capacitance) during scanning of the tip in DC-EFM. Since the capacitance between tip and sample is kept constant in the operation of DC-EFM, the domain image obtained from the ω component $(\partial C/\partial z V_{\text{dc}} + \sigma_b C/2\epsilon_0)$ in DC-EFM is well separated from the topographic image unlike the conventional noncontact EFM which frequently shows mixed image of topography and domain structure. To understand the origin of the image mixing, we will describe the effect of the electrostatic force gradient in the detection of ferroelectric domains by the noncontact mode EFM. As shown in Fig. 4, a large electric field gradient appears near the domain boundary where two opposite charge distributions meet. Furthermore for the tip-sample distance greater than 10 nm, for example, a significant force gradient appears along the lateral position. In the noncontact mode of EFM, the topography feedback loop adjusts the tip-sample distance in order to maintain constant vibration amplitude of the tip at resonance frequency of the cantilever. The electric properties of the sample can be simultaneously measured by applying dc and ac bias at another off-resonance frequency of cantilever. Therefore, in a noncontact EFM operation, the variation in the electrostatic force gradient due to the surface charge can shift a resonance frequency of probe oscillation, thus perturbing the topography measurement. In such a case, the probe tip follows a constant force gradient contour including the electrostatic force gradient as well as van der Waals force gradient. Thus the constant force gradient does not coincide with the real topography of the surface. However, in the operation of DC-EFM, the tip-sample distance is controlled by the repulsive atomic force instead of the force gradient. Thus the topography image is well separated from the electrical property of a surface.

Figure 5 shows topography and domain contrast images

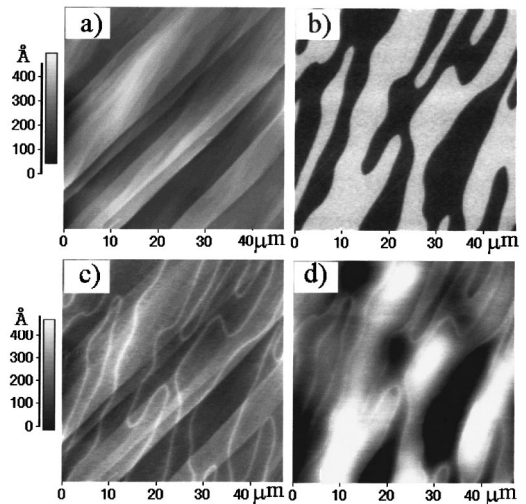


FIG. 5. Comparison the surface charge image obtained by DC-EFM and noncontact EFM. Images taken by DC-EFM do not show any correlation between topography (a) and surface charge (b) image. However, the images taken by noncontact EFM show a strong coupling between topography (c) and charge (d) image.

of TGS single crystal obtained simultaneously. Images are obtained by both DC-EFM and conventional noncontact mode EFM for the purpose of comparison. Cleaved TGS single crystal has 180° domains with the polarization direction perpendicular to the ac plane. Therefore the bound surface charge density $\sigma_b = \mathbf{P} \cdot \mathbf{n}$ of each domain is either positive or negative depending on the polarity. As shown in Figs. 5(a) and 5(b), topography and domain image, which are obtained by DC-EFM simultaneously, are well separated from each other. Domain contrast image shown in Fig. 5(b) shows sharply divided two distinct levels only as can be expected for 180° domains. However, topography [Fig. 5(c)] and surface charge image [Fig. 5(d)] obtained by the noncontact mode EFM show coupled or blurred images. In the topographic image, an enhanced contrast appears along the domain boundary where a strong electrostatic force gradient exists. In the noncontact operation, topography image is a convolution of van der Waals force gradient with electrostatic force gradient. Thus, the probe tip will show a constant force-gradient contour rather than a constant tip-sample separation contour. Domain contrast obtained by the noncontact operation [Fig. 5(d)] shows a much blurrier image, as if it is unfocused, compared to the one [Fig. 5(b)] obtained by DC-EFM. Yet we can distinguish the polarity for a wide domain. This grey level contrast can be explained by the behavior of the surface electric field as shown in Fig. 4. For a tip distance higher than 10 nm, the electric field changes gradually near the domain boundary. In addition, the electric field intensity over a narrow domain is much weaker than the one over a wide domain region. When the tip is far away from the surface, the electrostatic force exerted on the tip will be reduced by the decrease in the surface electric field intensity and also by the decrease of the induced charge on the tip due to decrease in the capacitance between the tip and electrode. Thus domain image shows a spatially averaged contrast, which in turn decreases the lateral resolution, therefore a contact operation such as in DC-EFM provides a better

domain contrast image as well as a better spatial resolution than a noncontact method. The advantage of DC-EFM compared to other similar methods such as the piezoresponse method¹³ or lateral force microscope¹⁴ for the detection of domain images is that it can provide a way for a quantitative evaluation of the surface charge density and a direct control of the domain structure in ferroelectric materials. In the nulling method, the feedback signal of the feedback controller controls V_{dc} such that the amplitude of ω component, $(\partial C/\partial z V_{dc} + \sigma_b C/2\epsilon_0)$, vanishes. The surface charge density is, therefore, related to the nulling dc voltage $V_{dc,n}$ as

$$\sigma_b = -2\epsilon_0 V_{dc,n}(\partial C/\partial z)/C. \quad (5)$$

Since DC-EFM is operated in a contact mode with the effective tip-sample distance d as small as 1 nm, the capacitance between tip and sample can be regarded as a parallel plate capacitor with the resulting $(\partial C/\partial z)/C \cong 1/d$. Thus, one can estimate the surface charge density of ferroelectrics directly from the nulling feedback signal in DC-EFM. If one applies a strong dc bias to the tip, a control of the domain structure (domain reversal) is also possible with DC-EFM.

IV. DISCUSSIONS

Electrostatic force modulation by applying an ac modulation bias between the tip and the electrode generates the vibration of the cantilever even in the contact state and also induces charges on the tip. The sustained vibration and the induced charge on the tip allows the detection of a weak electric force by a lock-in technique even in the presence of a strong atomic force at the surface.

Thus DC-EFM can be used either as a force modulation microscopy for the surface hardness, or as a potentiometry for the surface potential distribution, or as a charge densitometry for the ferroelectric domain study. Much better spatial resolution and clear detection of surface electrical properties can be achieved in DC-EFM than in the conventional non-contact EFM. Furthermore, topography, surface potential, and surface charge image are well separated from each other

in DC-EFM, that allows a quantitative evaluation of the bound surface charge density and control of the domain structure. For the quantitative evaluation of the surface charge density, however, it is required to measure the gap distance between tip and sample more accurately. In this work, we estimated the gap value from the force distance curve of the cantilever with an uncertainty of 10% which limits the accuracy of the estimated value of the surface charge density.

ACKNOWLEDGMENTS

This work was supported in part by the Nano-Structure Technology Project and also by the Ministry of Education in Korea under Grant No. BSRI-98-2416.

- ¹P. Maviald, H. J. Butt, S. A. C. Gould, C. B. Prater, B. Drake, J. A. Gurley, V. B. Elings, and P. K. Hansma, *Nanotechnology* **2**, 103 (1991).
- ²Y. Martin, D. W. Abraham, and H. K. Wickramasinghe, *Appl. Phys. Lett.* **52**, 1103 (1988).
- ³J. M. R. Weaver, D. W. Abraham, *J. Vac. Sci. Technol. B* **9**, 1559 (1991).
- ⁴A similar method based on the nulling condition of the force between tip and sample also yielded a simultaneous measurement of the topographic and surface potential. See, for example, M. Nonnenmacher, M. P. Boyle, and H. K. Wickramasinghe, *Appl. Phys. Lett.* **58**, 2921 (1991).
- ⁵J. E. Stern, B. D. Terris, H. J. Mamin, and D. Rugar, *Appl. Phys. Lett.* **53**, 2117 (1988).
- ⁶B. D. Terris, J. E. Stern, D. Rugar, and H. J. Mamin, *J. Vac. Sci. Technol. A* **8**, 374 (1989).
- ⁷F. Saurenbach and B. D. Terris, *Appl. Phys. Lett.* **56**, 1703 (1990).
- ⁸R. Luthi, H. Haefke, K.-P. Meyer, E. Meyer, L. Howald, and H.-J. Guntherodt, *J. Appl. Phys.* **74**, 7461 (1993).
- ⁹H. Bluhm, A. Wadas, R. Wiesendanger, K.-K. Meyer, and L. Szczesniak, *Phys. Rev. B* **55**, 4 (1996).
- ¹⁰J. W. Hong, Z. G. Khim, A. S. Hou, and S.-I. Park, *Appl. Phys. Lett.* **69**, 2831 (1996).
- ¹¹Y. Martin, C. C. Williams, and H. K. Wickramasinghe, *J. Appl. Phys.* **61**, 4723 (1987).
- ¹²J. W. Hong, K. H. Noh, S.-I. Park, S. I. Kwun, and Z. G. Khim, *Phys. Rev. B* **58**, 5078 (1998).
- ¹³A. Gruverman, O. Auciello, R. Ramesh, and H. Tokumoto, *Nanotechnology* **8**, A38 (1997).
- ¹⁴H. Bluhm, U. D. Schwarz, and R. Wiesendanger, *Phys. Rev. B* **57**, 161 (1998).